Back-supported stratified flame propagation in lean and nonflammable mixtures

Edouard Delangle, Bertrand Lecordier, Corine Lacour, Armelle Cessou

Back-supported stratified flame propagation in lean and nonflammable mixtures

Edouard. Delangle, Bertrand Lecordier, Corine Lacour, Armelle Cessou*

Normandie Univ., UNIROUEN, INSA Rouen, CNRS, CORIA, FR-76000 Rouen, France

Abstract

In an effort to reduce pollutant emissions and increase energy efficiency, partially premixed combustion has been integrated into many new combustion technologies. The present study investigated lean back-supported flames in a stratified combustion regime. Outwardly propagating flames were observed following ignition under laminar stratification conditions generated in a constant volume vessel. The quantitative analysis of the flame properties relied on simultaneous PIV measurements to obtain local flame burning velocities and stretch rates and used anisole-PLIF measurements to calculate the equivalence ratio. Simultaneous OH-PLIF and OH-gradient measurements were used to differentiate between the burned gas boundaries and the active flame front. This differentiation was necessary to investigate the nonflammable mixture. Simultaneous OH- and anisole-PLIF measurements were used to estimate the thermal flame thickness. Two flame families were investigated: in family A the flame was ignited in a lean mixture (φ=0.6) with a rich stratification; in family B the mixture in the chamber was nonflammable. In rich mixtures ignition compensated for the non-equidiffusive effects of the lean propane flame. Both a flammable and a nonflammable mixture were investigated to evaluate the time scales of the back-supported propagation for the given stratification. The enhanced combustion regime allowed the flame to propagate with an active flame front, even in the nonflammable mixture for a few milliseconds before the flame extinguished.

Introduction

In addition to providing a canonical description of premixed and nonpremixed combustion, many studies have addressed partially premixed combustion regimes, in which the oxidant and the fuel species are inhomogeneously mixed before reacting. These conditions are introduced intentionally to reduce pollutant emissions and increase energy efficiency in a variety of applications ranging from gas turbine combustors [1, 2] to stratified-charge direct-injection engines [3, 4].

Moreover, identical conditions are often encountered in practical devices in which the combustion regime involves mixture inhomogeneities (local extinction in two-phase combustion). Consequently, there is renewed interest in seeking a better understanding of partially premixed combustion, as reviewed by Masri [5]. The present paper examined stratified combustion in a premixed combustion regime with a compositionally inhomogeneous mixture in which the flame propagated successfully [5, 6]. For lean back-supported flames, stratified combustion results in a higher burning rate [7-9], active heat release [6], a reduced flame thickness [8], extended flammable limits [7, 10], and a better stretch resistance [11]. Experimental and numerical investigations have concluded that these effects occur because of increased temperature of burned gases and species flux from products [7, 12]. The present study experimentally investigated whether higher burning rates and thermal flame thinning enhance combustion. A time scale of these potential benefits is proposed for a lean back-supporting flame. The outwardly propagating flame configuration is a well-established and extensively used method for measuring burning velocities in homogeneous mixtures; the method is suitable for the direct determination of the stretch rate [13]. In this configuration, the burning velocity is often deduced from the flame speed (S_b) and the displacement speed of the burned gas, based on assuming a stationary burned gas and a known burned gas temperature. For inhomogeneous mixtures these assumptions are no longer valid, but the burning velocity [14] can be measured directly by determining the displacement speed with respect to the unburned gas U_n, defined as $S_b - U_g$ [15, 16], where U_g is the maximum velocity upstream of the flame. Here, outwardly propagating flames were observed following ignition under laminar stratification conditions generated in a constant volume vessel. The flame was first ignited in a richer mixture, and the analysis is conducted once the flame propagates in the lean homogenous mixture, as has been done previously [11]. This sequence was chosen to establish whether prior burning of a richer mixture affects the flame properties in the lean homogeneous mixture. The analysis was restricted to measuring flame segments that were primarily exposed to the curvature stretch effect with limited flow non-uniformity influences and with almost the same evolution from the point of ignition throughout the stratified mixture. The study used lean mixtures in which propane–air flames are sensitive to non-equidiffusive effects, which made it possible to also investigate flame stretch rates. As done previously, simultaneous PIV and anisole-PLIF measurements were used to analyse the flame properties [11]. Local flame burning velocities and stretch rates were derived from flame speed measurements, fresh gas velocities, and the principal curvature radii based on a PIV algorithm proposed in a previous paper [14]. The investigation of nonflammable mixtures requires burned gas boundaries to be differentiated from the active flame front. Simultaneous OH-PLIF measurements showed that the OH-gradient could be used to distinguish burned gas interfaces from active flame fronts.

Two flame families were investigated: family A, for which the flame was ignited in a lean mixture (φ = 0.6) with a rich stratification, corresponding to a mixture bordering on the flammability limit; and family B, for which the mixture in the chamber (φ = 0.4) was below the

* Corresponding author: armelle.cessou@coria.fr

flammability limit. Flames were also ignited in several richer mixtures ranging from $\varphi = 0.8$ to 1.5.

Balusamy et al. [11] have shown that the properties of back-supported stratified flames depend on the ignition conditions of the stratified layer. In richer mixtures, ignition compensates for the non-equidiffusive effects of a lean propane flame. The increase in flame propagation observed in lean homogeneous mixtures is caused as much by the flame's resistance to stretch as by an increase, in flame speed and burning velocity. The decay time of this influence of the stratification, called the memory [12], was determined in the present study. It is due to the fact that the flame properties are considered at the equivalence ratio in fresh gas, which differs from the effective equivalence ratio of the flame front (peak heat release) [6]. The back-supporting behaviour of the flame thus appears as a memory effect that reflects the amount of fuel previously consumed by the flame. Aiming to complement previous research [11], the present study used various mixture stratification amplitudes with both flammable and nonflammable mixtures to evaluate the flame's ability to propagate in these mixtures through a back support structure.

Experimental set-up

To investigate flame propagation in a laminar stratified mixture field, a constant volume combustion chamber was used in combination with PIV, anisole-PLIF, and OH-PLIF techniques.

Combustion facilities

Experiments were conducted in a 60×60×160 mm^3 constant volume combustion chamber equipped with three UV quartz windows. The chamber was initially filled with a lean homogeneous propane–air mixture with either $\varphi = 0.6$ or $\varphi = 0.4$ at atmospheric pressure. The stratified mixture field was created by injecting a laminar jet of a richer mixture into the chamber with an injection system, providing controllable and repeatable mixture stratifications. Two flame families were investigated (Tab. 1). The stratified mixture was spark-ignited by energizing two thin electrodes with a diameter of 0.4 mm placed at the centre of the combustion chamber. Previous experiments in this combustion chamber have shown that spark energy and electrode heat loss did not affect flame propagation. The limited volume of the chamber had little influence on flame propagation for the investigated time frame (pressure increase < 40 mbar), and due to the direct measurement procedure used for its determination, the burning velocity measurement is non-affected by the limited chamber volume [14].

		φ_{ig}			
	φ_{ch}	0.8	1.0	1.2	1.5
Family A	0.6			1.2–0.6	1.5–0.6
	0.7			1.2–0.7	
Family B	0.4	0.8–0.4	1.0–0.4	1.2–0.4	1.5–0.4

Tab. 1- Investigated flame families: mixture at rest in chamber (φ_{ch}); equivalence ratio at ignition (φ_{ig})

Laser diagnostics

The optical setup is presented in Figure 1. The PIV setup consisted of a double-cavity Nd:YAG laser (Twins Ultra, Quantel 30mJ@532nm), and CCD camera (Hamamatsu C9300 4Mp in 12 bits) that was equipped with a Nikkor lens (135mm, $f/d_{max} = 2$, f/8). The anisole-PLIF setup used a fourth harmonic generator with an Nd:YAG laser (Quantel, YG180) that delivered 30 mJ to ensure a linear regime. A dye laser (Quantel, TDL90 20 mJ) pumped by a second harmonic generator with an Nd:YAG laser (Quantel, Brillant B) was used as the OH-PLIF laser source. Both LIF radiation measurements were collected with ICCD cameras (Roper Scientific PIMAX512), equipped with a 98 mm UV lens (CERCO 2178, SODERN, f/2.8) for anisole-PLIF and a 105 mm lens (Nikkor 105, f/4.5) for OH-PLIF. Dichroic mirrors were used to optically combine the three laser beams, and the overlapping laser sheets were formed by combining a spherical (f = 1 m) lens with two cylindrical lenses (f = −25 mm, f = +100 mm).

The airflow was seeded with olive oil particles, and the propane flow was seeded with anisole (0.015% in volume in the stoichiometric propane–air mixture). OH–PLIF images were corrected for laser sheet inhomogeneities by collecting a LIF reference image obtained from homogeneous images of a rich propane–air mixture seeded with anisole. PIV and LIF radiations were separated with a dichroic mirror, which had a cut-off wavelength of 350 nm.

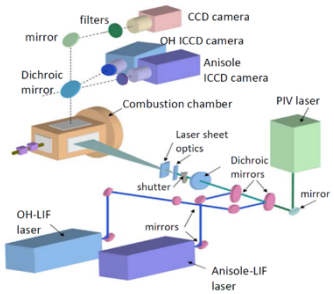

Figure 1: Experimental set-up

Fluorescence was collected for anisole in the spectral range of 275 to 350 nm with a 10 mm thick liquid filter (0.6% vol. of toluene in iso-octane) and with a combination of Schott filters (UG11 and WG280, 3 mm). The time delay between the two PIV pulses was adjusted to the velocity magnitude. The PLIF laser pulses were fired at intervals of 2 µs and positioned in the middle of the PIV time delay at intervals of 2 µs. A calibration grid was used to determine the high-order mapping functions of the three cameras. This calibration ensured the perfect overlap of the three measurements, especially for the OH-PLIF off-axis acquisition, which viewed the laser sheet at a slightly tilted angle, and is essential for providing a good accuracy of the flame thickness measurement described afterwards.

Active flame front identification

Once the flame reached the nonflammable mixture, $\varphi_{ch} = 0.4$, it became necessary to differentiate between the burned gas boundaries and the active flame front. For the

interface of fresh and burned gas, numerous studies have proposed to use OH-gradient levels to identify flame fronts [17-19]. After obtaining the OH outline, the OH signal was extracted along its normal. This normal profile was interpolated with a complementary error function (*erfc*) before calculating the noise-free gradient. To ensure that OH-gradient levels are suitable for determining active flame fronts, OH-gradient mapping was first compared with OH×CH2O PLIF to verify that this simple diagnostic was sufficiently able to localize local flame extinctions. This preliminary experiment is performed in a Bunsen burner conical flame, where a local extinction was produced by a small air jet. In Figure 2, a threshold value of OH-gradient is visible where the flame is extinguished. The value of this threshold value was determined for homogeneous outwardly propagating flame. The OH gradient has been measured for homogenous outwardly propagating flames at various equivalence ratios of up to φ = 0.6, while in the present configuration, the flame kernel could not self-propagate below φ = 0.62. Figure 3 shows the PDFs of the OH gradient according to equivalence ratio. The peak values decreased from the stoichiometric mixture to the lean composition. The flames with the two lowest equivalence ratios (φ = 0.6 and φ = 0.62) for which the homogenous flame could not self-propagate, presented PDFs clearly separated from the others. Thus, the critical threshold was defined as 17 000 a.u, after correcting the laser sheet profile.

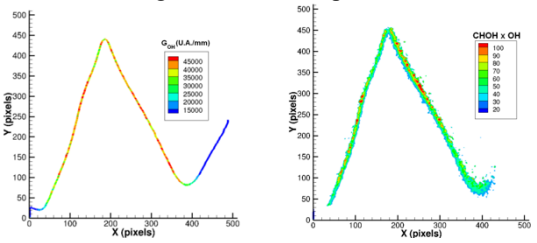

Figure 2: simultaneous OH-gradient and CH2OxOH LIF in a Bunsen burner conical flame, where a local extinction is made by injection a small air jet

Flame thickness determination

The equivalence ratio was measured based on anisole-PLIF, following a shot-to-shot laser sheet correction according to the procedure outlined by Balusamy et al. [11]. The OH-PLIF marked high temperature burned gas (T>1500 K), whereas anisole pyrolysis was noticeable around 800 K [20]. After calibrating the mapping functions of the three cameras, the distance between these two isotherms, determined by superpositioning the simultaneous OH-PLIF and anisole-PLIF measurements, was used to define a thickness labeled δ_{LIF}. The local distance between these two isotherms, which varies when flame has crossed stratification (Figure 4), is measured all around the flame outline from the superposition of the simultaneous OH-PLIF and anisole-PLIF.

Figure 5 shows a comparison of δ_{LIF} values obtained for different homogeneous flames with the thermal thickness $\delta_{th} = (T_b - T_u)/\nabla T_{max}$, calculated by modelling the unstretched 1D propane–air flame carried out by Cantera and the chemical scheme provided by Jerzembeck et al. [21]. The similarity of the resulting values shows that δ_{LIF} can be used to evaluate the local flame thickness.

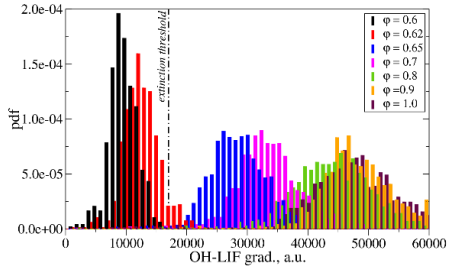

Figure 3 : PDF of OH-PLIF gradient normal to the PLIF outline

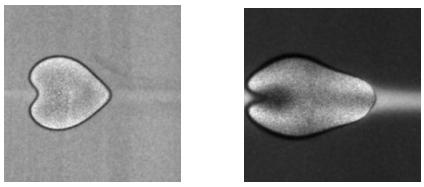

Figure 4 : superposition of the simultaneous OH-PLIF and anisole-PLIF for the homogeneous laminar jet at φ_{ig} = 0.8 to φ_{ch} = 0.8, (left) and for the case φ_{ig} = 1.2 to φ_{ch} = 0.4 (right), 4 ms after ignition

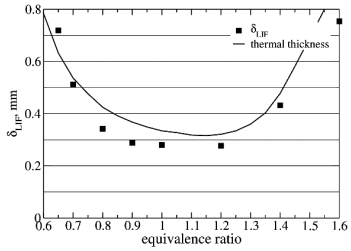

Figure 5 : Thickness according to equivalence ratio: comparison of δ_{LIF} with the thermal thickness given by the plane flame calculation for propane–air

These new measurements are combined with the measurements of burning velocity and stretch rates measured all around the stratified flames from the procedure of Balusamy et al [14], providing a direct measurement based on the difference between the local flame speed and the fresh gas velocity at the entrance of the preheat zone.

Results and discussion

The flame properties were analysed after the flame began propagating in the lean homogeneous mixture filling the combustion chamber that is, for $t \geq 2\ ms$. To limit the analysis to conditions comparable to outwardly propagating flames in a homogeneous mixture, the conditional analysis relied on the same criteria as used by Balusamy et al. [11]: Measurements were conditioned on the equivalence ratio in the chamber, ($\varphi_{ch} = \pm 0.05$) and the moderate tangential velocity (−5% to 5% of the U_g average). An additional condition limited the investigation to flame segments propagating almost perpendicularly to the stratified layer: an angular sector of ±20° from the ignition location was chosen (Figure 6). This angular condition restricted the flame analysis to

segments mainly exposed to the flame curvature effect with limited flow non-uniformity influences and with almost the same residence time in the homogeneous lean mixture. Given these new criteria, sampling was restricted to flame segments with an almost constant stretch rate at every moment after ignition. Consequently, the stretch rate was averaged at each time, and the flame properties were not extrapolated to a zero stretch rate, as done by Balusamy et al. [11].

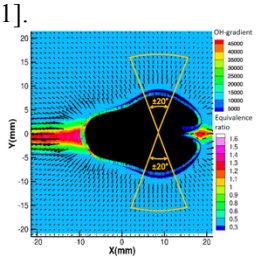

Figure 6 : Combined measurements and angular sector of the conditional analysis

Family A: propagation in the lean flammable mixture

Figure 7 presents the burning velocity according to time. For ignitions with φ_{ig} = 1.2 in family A at 0.34 m/s, the initial burning velocity of the flame segment propagating in the lean mixture (t = 2 ms) was significantly higher than expected for lean stretched flames with φ = 0.6 and 0.7: the unstretched velocity was $U_n^\circ = 0.12\ m/s$ for φ = 0.6 and $U_n^\circ = 0.20\ m/s$ for φ = 0.7. The stretch effect resulted in decreased burning velocities in lean propane–air mixtures. In the rich mixture, ignition initially led to high values of U_n, despite the high stretch rate (Figure 8).

For the two cases with φ_{ig} = 1.2, the velocity U_n showed identical time evolutions with an asymptotic trend of the exponential decrease for t > 6ms, where U_n was almost constant (Figure 7 and Figure 8). The asymptotic values were close to those of the unstretched velocity, with 0.20 m/s for φ_{ch} = 0.7, and 0.14 m/s for φ_{ch} = 0.6.

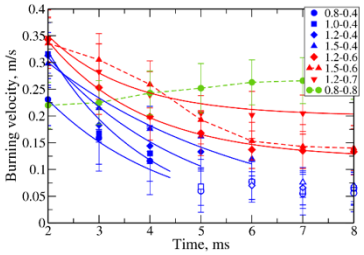

Figure 7. Burning velocity according to time: family A (red), B (blue), and homogeneous flames (green) with φ = 0.8. Extinguished flame conditions (open symbols).

Exponential modelling of $U_n(t)$ (Tab. 2), from t=2 ms to the asymptotic behaviour, shows that the decay time was $1.6\ ms$ for φ_{ch} = 0.7, and 1.9 ms for φ_{ch} = 0.7. The asymptotic behaviour was attained more rapidly for φ_{ch} = 0.6 because of the lower stratification amplitude (φ_{ig} = 0.6 to φ_{ch} = 0.7).

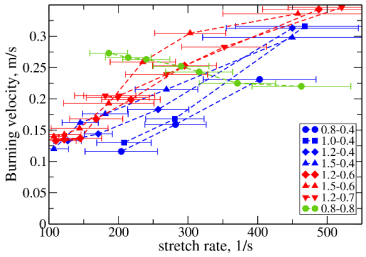

Figure 8. Burning velocity according to stretch rate

$$U_n(t-2) - U_\infty^\circ = (U_n(2ms) - U_\infty^\circ)e^{-\frac{t-2}{\tau}}$$

Family	$(\varphi_{ig} - \varphi_{ig})$	U_∞, m/s	$U_n(2\ ms)$, m/s	τ, ms
A	1.2–0.6	0.12	0.34	1.9
	1.2–0.7	0.2	0.35	1.6
B	1.5–0.4	0	0.3	4
	1.2–0.4	0	0.31	2.8
	1.0–0.4	0	0.32	2
	0.8–0.4	0	0.23	2.4

Tab. 2 - Exponential modelling of the burning velocity decay

Once the asymptotic behaviour was attained (t>5 ms), a slight increase in U_n was observed for φ_{ch} = 0.7 corresponding to the decreasing stretch effect observed for increasing flame radii. For φ_{ch} = 0.6, the minimum value of U_n was very close to the value of U_n°, and a slight decrease was observed, in agreement with previous observations by Balusamy et al. [11]. This behaviour illustrates the competition between the stretch effects, which tended to reduce the burning rate and the back-support behaviour of the flame. After igniting in the homogeneous mixture with φ_{ch} = 0.6, outwardly propagating spherical flames were no longer able to self-propagate due to overly intense stretch effects occurring with small flame radii. In the stratified case (φ_{ig} = 1.2 to φ_{ch} = 0.6) the flame succeeded to propagate despite its small radius, as confirmed by the OH gradient values (Figure 3), which were higher than the defined extinction threshold (17 000 a.u.). The flame was sustained by the memory effect, but was slowed down by the stretch effects. The gain provided by the memory effect decreased with time, and the influence of the stretch effect also decreased, resulting in a relatively constant burning velocity: for the investigated time range, the two effects were balanced, with a slightly faster decay observed for the memory effect.

Overall, these results show that ignition in a slightly rich mixture resulted in a flame that rapidly propagated in the lean mixture despite the high stretch rates. This velocity decreased as the flame propagated in the lean mixture, with a decay time of slightly less than 2 ms. This high burning velocity was related to the discrepancy between the local equivalence ratio in the flame front (peak heat release) and in fresh gas. The flame propagation then adopted an asymptotic behaviour with a burning velocity close to the fundamental velocity. The physical properties of the burned gas (here, mainly the high temperature) compensated for the non-equidiffusive effects of the lean stretched propane–air flame, which

resulted in a leaner mixture in front of the flame with a lower burned gas temperature.

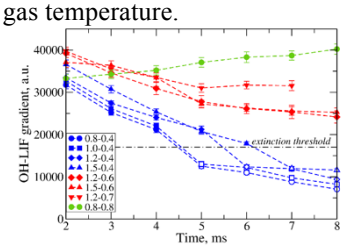

Figure 9. OH-PLIF gradient according to time

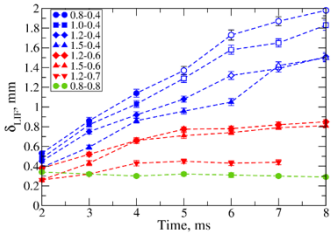

Figure 10. Flame thickness δ_{LIF} according to time

These observations were made for stratifications that led to few partial oxidation products in burned gas (peak equivalence ratio of 1.2). For φ_{ig} = 1.5 to φ_{ch} = 0.6 partial oxidation products are more abundant in burned gas. At 2 ms, just after the flame had left the stratified layer, U_n was equal to 0.33 m/s, which is roughly the same value as for φ_{ig} = 1.2 to φ_{ch} = 0.6 and for φ_{ig} = 1.2 to φ_{ch} = 0.7. Because stretching had an effect on the flame, these identical velocities possibly indicate either an identical equivalence ratio within the flame front for the three cases, or a much richer flame whose burning velocity was increased by the stretch effects. The time decay was slower and differed from the exponential decay observed for the two other cases of family A. The concavity of the curve $U_n(t)$ differed from the ignition cases with φ_{ig} = 1.2, demonstrating that the burning velocity increased more strongly between 3 and 6 ms. This additional combustion enhancement is visible in Figure 8, in which the case with φ_{ig} = 1.5 to φ_{ch} = 0.6 represents a faster burning velocity for stretch rates in a time range of 3 to 6 ms. These results show that the back-support behaviour of the flame was enhanced by ignition in a richer stratified layer: the excess in partial oxidation products in burned gas enriched the flame front for longer and/or led to a secondary reaction in the burned gas [23]. Due to the relative change in the curve concavity $U_n(t)$, a decay time cannot be determined through exponential modelling. However, the same asymptotic behaviour as for φ_{ig} = 1.2 to φ_{ch} = 0.6 was attained after a slightly longer time (t>6 ms); this behaviour was observed for all measured properties (Figure 7).

For the three cases of family A, the flame thickness δ_{LIF} showed the same time evolution. At t= 2 ms, despite the lean mixture in fresh gas, the flame was relatively thin with a thickness close to the minimum value measured in near-stoichiometric homogeneous flames for the cases φ_{ig} = 1.2 to φ_{ch} = 0.7 and φ_{ig} = 1.5 to φ_{ch} = 0.6 the flame was slightly thicker for the case φ_{ig} = 1.2 to φ_{ch} = 0.6 with $\delta_{LIF} = 400\ \mu m$, corresponding to φ = 0.85 for a homogeneous flame (Figure 9). These smaller thickness values are consistent with high values of U_n. Then, δ_{LIF} increased over time to attain a roughly constant value close to that measured in the homogeneous flame with φ_{ch} = 0.6 and 0.7 (Figure 5).

Family B: propagation in a lean nonflammable mixture

Flames of family B, for which the lean mixture was below the flammability limit, were investigated to determine whether this combustion enhancement also occurred in nonflammable mixtures and over which time scales. For these four flames, the OH-LIF gradient was used to differentiate the border of hot burned gas from the active flame front (Figure 9). At t=2 ms the OH-LIF gradient values were much higher than the extinction threshold (17 000 a.u./mm). Depending on the stratification amplitude, the gradient's progressive decay and the extinction occurred at different times greater than 4 ms and increased with the equivalence ratio at ignition. Thus, ignition in a richer stratified mixture allowed the flame to propagate in the nonflammable mixture: the flame ignited in the lean mixture (φ_{ig} = 0.8) as well as in the rich mixture (φ_{ig} = 1.5). Figure 7 shows the burning velocities over time for active reaction zones (with an OH-LIF gradient higher than 17 000 a.u/mm). The conditions for which the flame extinguished (open symbols in Figure 7), indicate that the burning velocity was non-zero due to measurement inadequacies in this case. At 2 ms, the case φ_{ig} = 0.8 to φ_{ch} = 0.4 had a burning velocity of 23 cm/s, a value close to the velocity measured for φ_{ig} = 0.8 to φ_{ch} = 0.8 (Figure 7), which is evidence of enhanced combustion in the nonflammable mixture. This increase was observed even if the flame was ignited in a lean stratified layer (peak equivalence ratio of 0.8). In this case, enhanced combustion could only have resulted from an increase in the burned gas temperature. This enhancement decreased over time, and flame extinction occurred between 4 and 5 ms. The three other flames (φ_{ig} = 1.0 to φ_{ch} = 0.4; φ_{ig} = 1.2 to φ_{ch} = 0.4 and φ_{ig} = 1.5 to φ_{ch} = 0.4) had nearly identical burning velocities of around 0.3 m/s at 2 ms. The burning velocities decreased over time; the slowest decay time was observed with the richer stratification. Exponential modelling of the decay with $U_\infty = 0\ m/s$ took into account the extinction occurrence. The following decay times were determined: 4 ms for φ_{ig} = 1.5 to φ_{ch} = 0.4; 2.8 ms for φ_{ig} = 1.2 to φ_{ch} = 0.4; and 2 ms for φ_{ig} = 1.0 to φ_{ch} = 0.4 (Tab. 2). For φ_{ig} = 0.8 to φ_{ch} = 0.4 the decay time was slightly longer (2.4 ms), or at least roughly equivalent, considering the measurement uncertainty. This result demonstrates the combined effects of stretch and stratification. For rich propane–air mixtures, stretching tended to increase the burning velocity. Thus, in these cases, combustion was enhanced by both stratification and stretching, which led to higher burned gas temperatures. During propagation in the lean mixture, these positive influences decreased simultaneously. For ignition in the lean mixture with φ_{ig} = 0.8 to φ_{ch} = 0.4, the burned gas temperature increased as a result of ignition in the stratified mixture, whereas stretch tend to decrease this temperature. During

propagation in the lean mixture, the effect of stretch on combustion decreased progressively, leading to a slower decay. However, the increase in decay time remained moderate, and the flame was rapidly extinguished (t<5 ms) because of the minor presence of a back-support structure for the stratification in this case.

The combustion enhancement was also noticeable with the small values of δ_{LIF} at 2 ms (Figure 5). The flame thickness was around 500 µm, and was as thin as 400 µm for φ_{ig} = 1.5 to φ_{ch} = 0.4. These values are close to the value measured in a homogeneous flame with φ = 0.8. The flame became thicker over time, and extinction occurred at $\delta_{LIF} > 1.2\ mm$. For the entire duration, the richer the stratification was, the thinner the flame became. Additionally, for a given stretch rate, the fastest burning velocity occurred in the richer stratification (Figure 8). These results show that a richer stratification resulted in longer lasting, increasingly enhanced combustion in the lean nonflammable mixture.

Conclusion

Simultaneous PIV, anisole-PLIF, and OH-PLIF measurements were used to experimentally investigate the possibility of lean-burn combustion. Outwardly propagating flames were ignited under laminar stratification conditions generated in a constant volume vessel. After ignition in a rich stratified layer, the flame properties (burning velocity, stretch, thermal thickness δ_{LIF}) were analysed in a lean flammable mixture bordering on the flammability domain (family A) and in a nonflammable mixture (family B).

The behaviour of flames in family A showed that the lean-mixture flames benefited from ignition in the rich stratified layer, which led to faster burning velocities despite the high stretch rate that usually inhibits combustion in such a lean mixture ($\varphi = 0.6$). The burning velocity decreased toward fundamental values, with a decay time close to 2 ms for the investigated configuration. The memory effect compensated for the stretch effect, resulting in a fundamental burning velocity at a non-zero stretch rate. For family B, the flame maintained an active flame front in the nonflammable mixture over time, which increased with the equivalence ratio in the stratification. The combustion enhancement was also apparent in the flame thickness values δ_{LIF}: the flame became thinner in the early stage of propagation in the lean mixture. The thickness values were depended on the effective equivalence ratio in the flame front and on the flame thickness, whereas the burning velocity decreased. Stratified flames were used to construct a database suitable for validating numerical simulations and investigating the influence of—in contrast to homogeneous combustion—higher burned gas temperatures and excess in partial combustion products, which could enrich the flame front and compensate for the negative thermodiffusive effects of the lean propane flame (Le<1).

Acknowledgment

We gratefully acknowledge the support of the French *Agence Nationale de la Recherche* [National Research Agency] (ANR) and the French *Centre National de la Recherche Scientifique* (CNRS) through the ACTING-CO2 program, provided in collaboration with the French engine research grouping *Groupement Scientifique Moteurs* (GSM). We would like to thank Dr G. Lartigue for his help in modelling and for the fruitful discussions.

References

1. Huang Y, Yang V. Progress in Energy and Combustion Science. 2009;35(4):293-364.
2. Gicquel LYM, Staffelbach G, Poinsot T. Large Eddy. Progress in Energy and Combustion Science. 2012;38(6):782-817.
3. Yang Y, Dec JE, Dronniou N, Sjöberg M. Tailoring. Proc Comb Inst. 2011;33(2):3047-55.
4. Zhao F, Lai MC, Harrington DL. Progress in Energy and Combustion Science. 1999;25(5):437-562.
5. Masri AR. Proc Comb Inst. 2015;35:1115-36.
6. Zhou RG, Hochgreb S. Combust Flame. 2013;160(6):1070-82.
7. Marzouk YM, Ghoniem AF, Najm HN. Proc Comb Inst. 2000;28(2):1859-66.
8. Richardson ES, Granet VE, Eyssartier A, Chen JH.. Combustion Theory and Modelling. 2010;14(6):775 - 92.
9. Jiménez C, Cuenot, B., Poinsot, T., Haworth, D., Combust Flame. 2002;128(0):1-21.
10. Kang T, Kyritsis DC., Proc Comb Inst. 2007;31(1):1075-83.
11. Balusamy S, Cessou A, Lecordier B. Combust Flame. 2014;161(2):427-37.
12. Pires da Cruz A, Dean, A.M., Grenda, J.M., Proc Combust Inst. 2000;28(0):1925-32.
13. Egolfopoulos FN, Hansen N, Ju Y, Kohse-Höinghaus K, Law CK, Qi F., Progress in Energy and Combustion Science. 2014;43(0):36-67.
14. Balusamy S, Cessou A, Lecordier B., Experiments in Fluids. 2011;50(4):1109-21.
15. Andrews GE, Bradley D., Combust Flame. 1972;19(2):275-88.
16. Bradley D, Gaskell, P.H., Gu, X.J., Combust Flame. 1996;104(0):176-98.
17. Sadanandan R, Stöhr M, Meier W., Applied Physics B. 2008;90(3-4):609-18.
18. Sweeney M, Hochgreb S., Appl Opt. 2009;48(19):3866-77.
19. Bayley AE, Hardalupas Y, Taylor AMKP, editors., 15th Int Symp on Applications of Laser Techniques to Fluid Mechanics; 2010; Lisbon, Portugal.
20. Nowakowska M, Herbinet O, Dufour A, Glaude P-A., Combust Flame. 2014;161(6):1474-88.
21. Jerzembeck S, Peters N, Pepiot-Desjardins P, Pitsch H., Combust Flame. 2009;156(2):292-301.